ELSEVIER

Journal of Power Sources 81–82 (1999) 480–486

JOURNAL OF POWER SOURCES

www.elsevier.com/locate/jpowsour

Interrelation between structural and electrochemical properties of the cathode based on vanadium oxide for rechargeable batteries

E. Shembel [a], R. Apostolova [a], V. Nagirny [a], D. Aurbach [b,*], B. Markovsky [b]

[a] *Ukrainian State Chemical Technology University, 320005 Dniepropetrovsk, Ukraine*
[b] *Department of Chemistry, Bar-Ilan University, Ramat-Gan, 52900, Israel*

Abstract

An electrochemical method for the anodic synthesis of active electrode materials based on vanadium oxides (electrochemically synthesized vanadium oxides—ESVO) in an aqueous vanadyl sulfate solution, has been evaluated with the main goal of optimizing the electrochemical performance of these materials as cathodes in lithium batteries. The influence of synthesis conditions and the regime of the subsequent thermal treatment of the vanadium oxide on its structural characteristics and electrochemical performance in non-aqueous electrolyte systems have been investigated. The study included the use of EC, DMC/$LiPF_6$ and PC, DME/$LiClO_4$ electrolyte solutions with two types of electrodes: (a) a vanadium oxide film deposited directly on a conducting substrate (stainless steel grid) by electrolytic synthesis, and (b) a composite electrode consisting of vanadium oxide, graphite or carbon black additives and a binder. The results of potentiodynamic and galvanostatic investigations obtained with these electrodes during cycling were highly reproducible, indicating good reversibility of the electrodes. Correlation between structural characteristics of the ESVO electrodes, their electrochemical responses and the evolution of the chemical diffusion coefficient of Li-ion with the state-of-discharge has been established and discussed.

Keywords: Lithium batteries; Vanadium oxide cathodes; Structural characteristics; Electrochemical behavior; Li-ion diffusion coefficient

1. Introduction

Vanadium oxides as cathodes for lithium batteries have for many years been a subject of great interest for investigators [1–14] because of the high specific discharge characteristics of these materials. As has been stated in recent publications [15,16], vanadium pentoxide is a very promising cathode for Li batteries since, in the presence of this electrode, the lithium surface is covered by a film providing high cyclability.

Many synthetic methods are used for vanadium oxide preparation. Among them are the gel method and its modification [6,17–20], a method based on ozone oxidation [10], electrophoretic deposition [12], r.f. sputtering [8] and film sputtering by physical vaporization [14], a spin-coating technique for fabrication of a new 2D-structure vanadium oxide by thermal decomposition of NH_4VO_3 [21], a rapid quenching technique [22], a fusion of mixtures of V_2O_5 and P_2O_5 [12], etc.

In our previous work [23,24], we outlined the prospects of the electrochemical synthesis of vanadium oxides. It should be mentioned that the electrochemical method of synthesis allows one to regulate and control the conditions of the synthesis, and to obtain products with predetermined characteristics. In addition, the electrodes obtained by electrochemical synthesis directly onto a metal substrate are of special interest for investigating the mechanism of an electrochemical process uncomplicated by macrokinetics inherent in the systems with conducting additive and a binder.

There are data on the cathodic synthesis of vanadium oxides from ammonium metavanadate NH_4VO_3 solutions [12], and anodic synthesis from vanadyl sulfate solutions $VOSO_4$ [25]. However, some problems relating to the electrochemical synthesis of vanadium oxides still remain unresolved. They relate mainly to the stability of the electrolyte, quality and composition of the deposits, and their adhesion to the substrate.

Much attention has been paid to comparing the properties of amorphous and crystalline samples of vanadium oxides [15,16,25,26], as well as to the identification of

* Corresponding author. Tel.: +972-3-531-8317; Fax: +972-3-535-1250; E-mail: aurbach@ashur.cc.biu.ac.il

0378-7753/99/$ - see front matter
PII: S0378-7753(99)00206-2

phase transitions during Li intercalation/deintercalation process [7,10,27–30]. The influence of thermal treatment of the vanadium oxides on the formation of their crystalline structure was pointed out [8,18,26]. Authors [27] demonstrated that Li-ion chemical diffusion coefficient D into the cathode bulk is higher for an amorphous vanadium oxide than for a crystalline one. It was shown [10] that *D* values changed only slightly in the discharge process with an amorphous V_2O_5 cathode, but there were extrema on the *D*–potential curve in the case of a crystalline sample. One important question still remains answered concerning the diffusion coefficient of Li-ions into the vanadium oxide matrix. Several techniques have been proposed for the evaluation of the diffusion coefficient, although the values of *D* for the same material reported by different research groups may differ by several orders of magnitude [8,17,19,22]. In the present study, we measured the diffusion coefficient of Li-ion for ESVO samples obtained under the same conditions, the only difference being the subsequent thermal treatment of the samples; *D* values have been estimated using potentiostatic intermittent titration and galvanostatic intermittent titration techniques (PITT and GITT, respectively).

The main goals of the present paper are as follows: (1) elucidation of the electrochemical method of obtaining vanadium oxides, providing high stability of aqueous vanadyl sulfate solution and predetermined characteristics of the ESVO; (2) investigation of the interrelationship between the conditions of the electrochemical synthesis of the vanadium oxide compounds, their structural properties, transport characteristics of Li-ion in the course of intercalation with vanadium oxide cathode, and its charge–discharge performance in non-aqueous electrolyte solutions; (3) evaluation of the possibility of phase transitions in cathodes based on ESVO using a combination of physical and electrochemical techniques.

2. Experimental

2.1. Preparation of electrodes

The electrochemical method of anodic synthesis of vanadium oxides from vanadyl sulfate solution in potentiostatic conditions on a gold electrode is described [26]. In our work, the oxide synthesis was carried out galvanostatically onto a stainless steel grid, thus providing desirable technological parameters of the process. The solution composition and the parameters of the synthesis should provide electrolyte stability, high quality of the deposit, its adhesion to the substrate, etc. A vanadyl sulfate solution was prepared from the mixture of V_2O_3, oxalic and sulfuric acids, and then subsequently electrolytically treated. The following factors were taken into account for optimizing the synthesis conditions, namely the anodic evolution of oxygen, reduction at the cathode of some vanadium compounds from the solution, the influence of pH both on the quality of the oxide deposit and corrosion resistance of steel. The optimal conditions of the electrochemical synthesis of vanadium oxide are as follows: vanadyl sulfate concentration range of 0.1–0.35 M/l; current density of 7.5–12.5 mA/cm^2; pH of 1.5–1.8; temperature of 80–85°C. Both compact and dispersed deposits were obtained on a stainless steel substrate.

ESVO samples were thermally treated at various temperatures (100–550°C, up to 7.5 h). Some samples were dried at ambient temperature for 24–48 h, then stored in propylene carbonate (PC) and in a non-aqueous electrolyte solution for 24 h in order to remove traces of water. For preparation of thin electrodes, the powder was admixed with carbon black (10 w/o) and PVDF (Aldrich) binder (10 w/o) in *N*-methyl-pyrollidone (Fluka). The slurry was then uniformly spread on both sides of an aluminum foil current collector and dried at 125°C. The active mass of the electrode was 1.8 mg. A battery grade electrolyte solution from Merck was used (1 M $LiPF_6$ in a mixture of ethylene carbonate (EC) and dimethyl carbonate (DMC), volume ratio (1:3)). The electrolyte solution comprising PC, dimethoxy ethane (DME) and $LiClO_4$ (Sinteka) was also used. The water content in electrolytes was about 20 ppm.

2.2. Cells and instrumentation

Electrochemical experiments were carried out in three-electrode polyethylene or glass cells with lithium foil and lithium wire serving as counter and reference electrodes, respectively. For galvanostatic cycling, a sandwich-type two-electrode cell was used. Cell assembly was performed in a glove-box filled with pure dry argon (oxygen level less than 10 ppm). Electrochemical impedance spectroscopy (EIS) measurements were carried out in the 200 kHz–5 mHz frequency range on a cell at open-circuit voltage conditions. Instrumentation included a Schlumberger model 1286 electrochemical interface and model 1255 frequency response analyzer driven by Zplot software from Scribner Ass. Cyclic voltammetry and PITT data were obtained using EG&G potentiostat (model 273, Echem software) coupled with 486 PC. For galvanostatic cycling experiments, a computerized multichannel Maccor-2000 battery tester was used. Electrochemical measurements were carried out with the help of a potentiostat PI-50-1.1, programmer PR-8 and a PDA registration device. The experiments were thermostatted at 25 ± 0.5°C.

The specific surface area of the vanadium oxide powder was determined by the BET method (Micromeritics, Gemini 2375 Instruments). SEM characterization of the materials was performed using a scanning microscope JEOL-JSM 840. The XRD measurements were performed using a DRON-2 diffractometer (CuKα, 35 kV, 10 mA). For TGA

studies the Q-1500D was used (heating rate of 15°C/min, vanadium oxide powder sample of 80–160 mg). The DSC analysis was performed using a Mettler DSC 25 instrument. Auger-electron spectra were obtained with a 09-IOS-10-005 spectrometer. The surface of the oxide sample was cleaned with Ag^+ ions (3 kW, ion density flow of 150 $\mu A/cm^2$) prior to the measurements. IR absorption spectra were obtained using a Specord-75IR spectrometer (KBr matrix).

3. Results and discussion

3.1. Morphological and structural investigations

Fig. 1 shows typical SEM photographs of the ESVO. It can be seen that the oxide grows on the substrate in the form of separated agglomerates, 10–15 μm in size (Fig. 1a). Fig. 1b and 1c compare a compact ESVO deposit on a stainless steel grid with that of ESVO powder (the latter obtained during prolonged electrolysis). They both reveal the similar surface sponge-like structure, but in the case of powder the surface is highly developed. ESVO samples obtained in the form of compact deposits and powder were black in color. The specific surface area of the powder was 1.4 m^2/g. The XRD pattern (Fig. 2) of vanadium oxide electrochemically synthesized and stored in the air for about 48 h exhibits a mixture of dispersed crystalline (ca. 130 Å crystallites size) and amorphous phases. We can assume the existence of vanadium oxides of the general formulae of V_2O_x ($x = 4.3–5.0$), obtained by electrochemical synthesis. According to the results of TGA and DSC studies of this oxide sample, the decrease in its mass at 110°C and 390°C, and the endothermic effect of the reaction are probably due to the loss of free and structurally bonded water (0.75 mol and 0.15 mol H_2O, respectively, per 1 mol of V_2O_5). The Auger-electron spectroscopic analysis of the thermally treated (300°C, 2.5 h) vanadium oxide sample reveals a non-stoichiometric composition corresponding to $VO_{2.2}$. The oxygen deficit in an electrochemically synthesized vanadium oxide sample thermally treated at $t < 300$°C was proven by the IR-spectroscopy data. It can be concluded that the character of the chemical bond in the oxide differs from that of V_2O_5 in the range of 1100–500 cm^{-1}. The absorption bands of the V–O bond (995, 753, 540) are shifted to the short wave region when compared with V_2O_5, thus proving the oxygen deficit.

The more intensive thermal treatment (350°C, 5.5 h or 450°C, 1–3 h) leads to color changes of the samples (from black to yellowish-brown) and the corresponding changes of their XRD characteristics. The XRD patterns of these thermally treated vanadium oxides obtained by electrochemical synthesis correspond to the crystalline V_2O_5 with the following parameters of the orthorhombic syngonia cell: $a = 11.51$ Å, $b = 3.559$ Å, $c = 4.371$ Å. Attention should be paid to the observed coincidence between the major intensive diffraction peaks in the XRD patterns of both the non-treated and thermally treated vanadium oxides. At the same time, there is a shift of the most intensive line (110) to larger scattering angles which can be attributed to the decreasing ($d = 0.12$ Å) of the interlayer distance d_{110}, probably due to the H_2O losses. XRD peaks related to the thermally treated ESVO (Fig. 2) are more pronounced than those presented in [26], thus indicating that our samples possess a much higher degree of crystallinity.

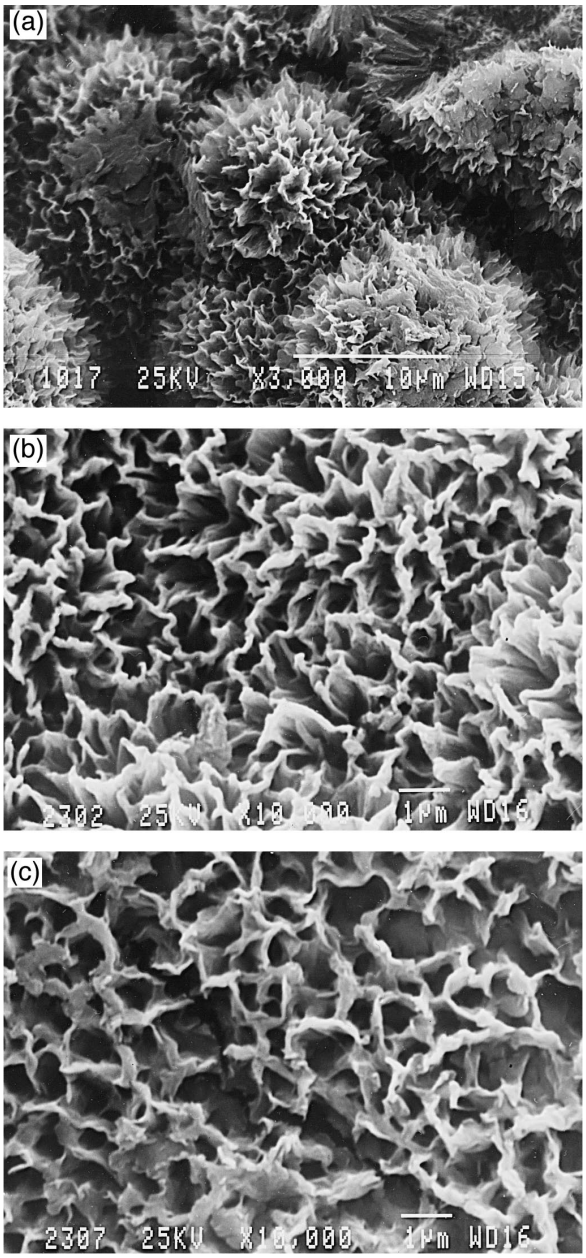

Fig. 1. SEM micrographs of the electrochemically synthesized vanadium oxides (ESVO). (a,b) Compact deposit onto a stainless steel grid; (c) powder obtained during prolonged electrolysis onto a flat stainless steel plate.

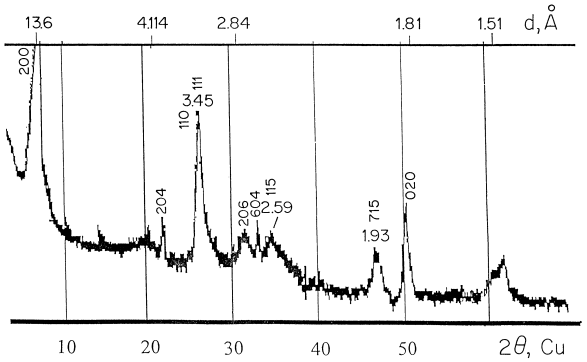

Fig. 2. XRD pattern of the ESVO powder dried for 48 h at ambient temperature.

The following observations can be drawn from the comparative analysis of the data obtained in the present study and from the literature, on the influence of the bonded H_2O in vanadium oxide upon its structure: for amorphous aerogel [5] $V_2O_5 \cdot 0.5H_2O$ peak 001 corresponds to $2\theta = 9.6°$, $d = 9.2$ Å; for xerogel [5] $V_2O_5 \cdot 0.6 H_2O$ $d = 12.5$ Å; for xerogel dried in the air [6] $d = 11.20$ Å; $VO_{2.2} \cdot 0.9H_2O$, electrochemically synthesized in our work, is characterized by parameter $d = 13.6$ Å at small scattering angles of $2\theta = 7.5°$. Thus, the bonded water molecules lead to an increase in the interlayer distance in vanadium oxides obtained by different techniques.

3.2. Electrochemical studies

The potentiodynamic responses of the cathodes based on ESVO of type (a), non-thermally treated, and those after 300°C, 2.5 h treatment, are very similar, and reveal two pairs of well defined anodic and cathodic peaks (Fig. 3; peak potentials are indicated). As can be seen, the more intensive thermal treatment (300°C, 7.5 h) of the oxide samples leads to a potential shift of the voltammetric peaks to more positive values, and a new redox couple appears.

The cyclic voltammogram obtained at a scan rate of 0.5 mV/s with the thermally treated (450°C) electrode is very similar to that of the composite electrode comprising crystalline orthorhombic V_2O_5, carbon black conducting additive and a binder.

It should be noted that a type (a) vanadium oxide electrode exhibits good reversibility in long-term cycling (Fig. 3b). We assume that the Li intercalation/deintercalation process in a potential range of 2.2–4.0 V vs. Li/Li^+ occurs without substantial changes of the solid phase oxide structure. Galvanostatic cycling experiments performed with a thermally treated (300°C, 7.5 h) ESVO electrode demonstrated a discharge capacity of 144 mAh/g at $I = 0.05$ mA/cm^2 against 107 mAh/g for the non-treated electrode. This fact, however, does not correlate with the data obtained by Sato et al. [26]. We assume that the parameters of the electrochemical synthesis of vanadium oxides elucidated in our work enabled the preparation of cathode materials with high discharge characteristics.

Two kinetic parameters, namely, the chemical diffusion coefficient of Li-ion in the cathode bulk and the total resistance of the intercalation process derived from impedance measurements, were obtained in this work. The chemical diffusion coefficient values were calculated using both the PITT and GITT methods as is described elsewhere [31–33]. The diffusion length was evaluated to be 3 μm in our case, according to SEM observations.

Fig. 4 demonstrates $-\log D$ vs. E functional relationships obtained for vanadium oxide electrodes with a different thermal treatment prehistory. The chemical diffusion coefficient remains almost constant in a 3.7–2.6 V potential range in the case of a thermally non-treated electrode with the increased amount of amorphous phase (Fig. 4a).

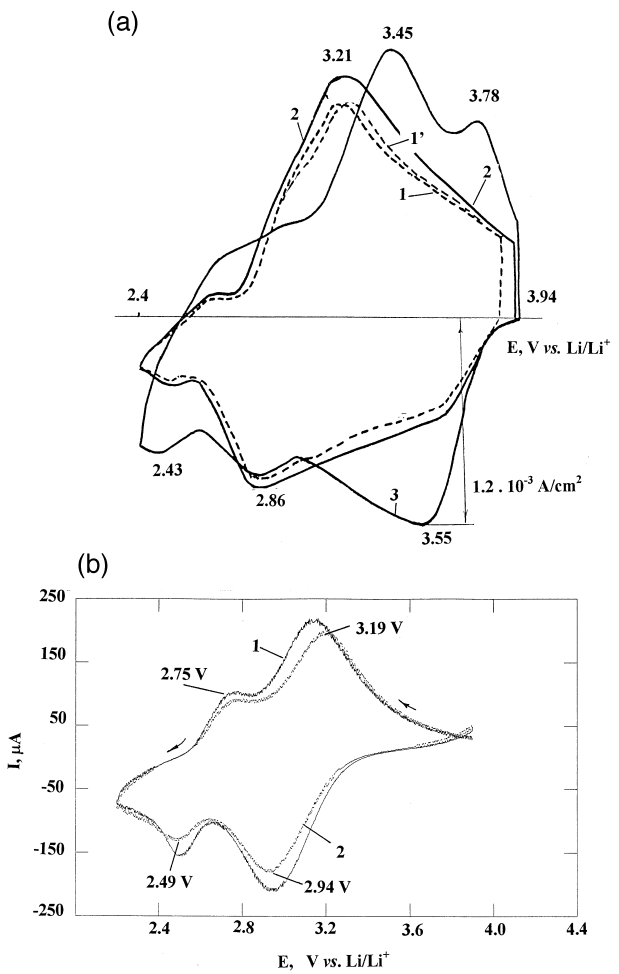

Fig. 3. (a) Cyclic voltammograms measured with cathode based on ESVO. Thermal treatment: (1) 18°C, 48 h; (2) 300°C, 2.5 h; (3) 300°C, 7.5 h; electrode active mass 4.0 mg/cm^2; potential scan rate 0.5 mV/s; Electrolyte: PC, DME, $LiClO_4$. (b) Cyclic voltammograms obtained at a scan rate 0.5 mV/s in EC, DMC, $LiPF_6$ electrolyte solution with cathode based on the ESVO. Thermal treatment: 300°C, 2.5 h; (1) first scan with a fresh electrode; (2) after 20 galvanostatic cycles.

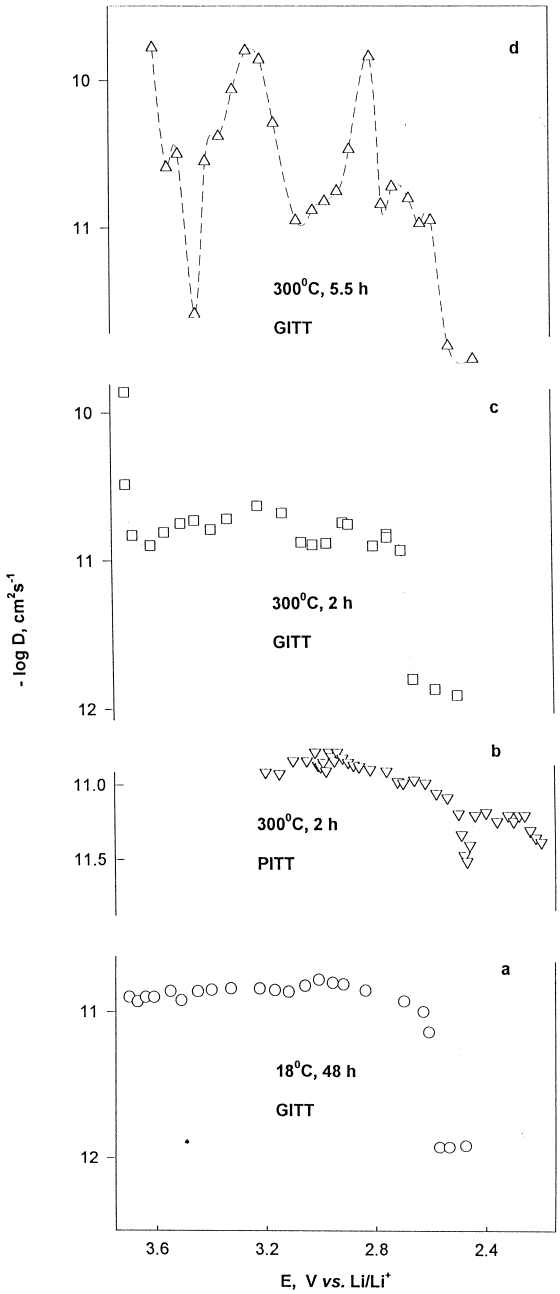

Fig. 4. Evolution with potential of the chemical diffusion coefficient of Li ions in the course of intercalation of the ESVO cathode. Substrate–stainless steel grid. Electrolyte: (a, c, d) PC, DME, $LiClO_4$; (b) EC, DMC, $LiPF_6$. Thermal treatment conditions and electrochemical technique used are indicated.

Only at a discharge potential of 2.6 V ($x \rightarrow 1$ in $Li_xV_2O_5$) is there a pronounced decrease of D values up to 10^{-12} cm^2/s.

It should be pointed out that the correlation between Li diffusion coefficient behavior and the structural characteristics of ESVO depend strongly on the conditions of the thermal treatment of the electrodes. As the thermal treatment time increases (at the same temperature of 300°C) and the oxide structure becomes similar to that of crystalline V_2O_5, the diffusion coefficient evolution becomes complex and has extrema (Fig. 4c,d) that are more pronounced when the thermal treatment time is larger. The diffusion coefficient values obtained by GITT and PITT measurements correspond well with each other (Fig. 4b,c).

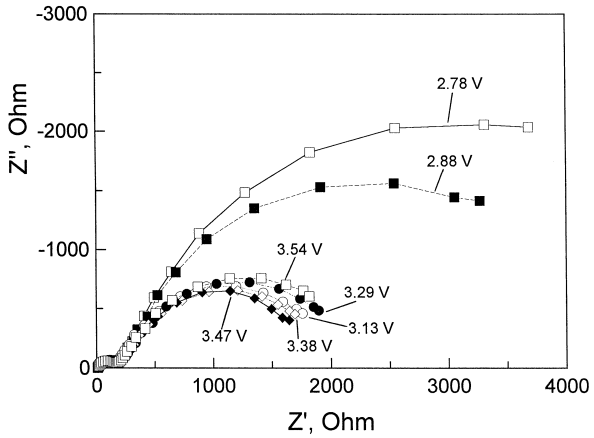

Fig. 5. A family of Nyquist plots measured with thin electrode based on the ESVO, carbon black and PVDF binder. Substrate–aluminum foil. Deintercalation of Li-ions. Equilibrium potentials are indicated. Electrode active mass was 1.8 mg/1.6 cm^2.

Diffusion coefficient values at the discharge potential of about 2.4–2.5 V for the ESVO electrode in an EC, DMC, $LiPF_6$ electrolyte solution (Fig. 4b) correspond well with those presented in Fig. 4c (EC, DME, $LiClO_4$ system). As seen from the above data, there is no substantial influence of the electrolyte solution compositions studied upon lithium transport in the cathode bulk.

From the analysis of the data obtained, we can conclude that there is an important correlation between the diffusion coefficient evolution ($-\log D$ vs. E), CV responses and

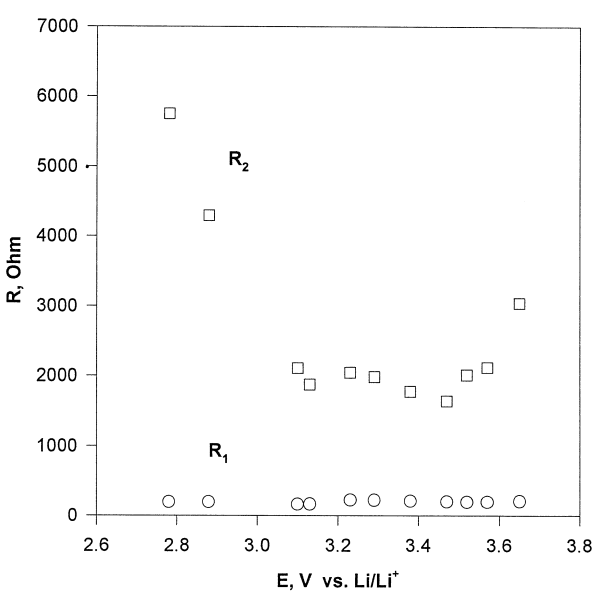

Fig. 6. Potential dependence of the resistance corresponding to the 1st and 2nd semicircles derived from the impedance plots of Fig. 5.

structural characteristics of the ESVO electrodes. Intercalation potentials at which D values are minimal (Fig. 4b,c,d) correspond well to the cyclic voltammetry peaks (Fig. 3a,b). Such a correlation has been observed for Li-transition metals oxide ($LiNiO_2$, $LiCoO_2$, $LiMn_2O_4$) intercalation systems [33–35], and can be explained in terms of phase transitions and interactions between the intercalated ions in the host matrix.

Fig. 5 presents the electrochemical impedance data (expressed as Nyquist plots) of a thin composite electrode (ESVO, carbon black and PVDF on the Al foil current collector) during the course of deintercalation at different equilibrium potentials. The spectra clearly reflect a combination of two semicircles in high and high-to-intermediate frequency domains, respectively. The resistance R_1 corresponding to the high-frequency semicircle changes only slightly in the range of 2.75–3.75 V (Fig. 6). We assume that R_1 represents the resistance of the lithium ion transport through the surface layer formed on the composite electrode due to its interactions with the electrolyte. Fig. 6 demonstrates that the resistance R_2 of the high-to-intermediate frequency semicircle is strongly potential dependent, and to our opinion, it reflects mainly the process of the interfacial charge-transfer. The Warburg impedance for diffusional transport of the intercalated ions was not observed for this electrode. Most probably, the Warburg region lies in the very low frequencies domain (< 0.005 Hz), as is in the case of the $Li_{1-x}NiO_2$ electrode [36].

When comparing the evolution with potential of R_2 impedance characteristic, the slow scan rate CV of this electrode, and the relationship $-\log D$ vs. E, we conclude that there is an interesting correlation between them. Namely, the extrema in the $-\log D$ vs. E plot are very close both to the CV peak potentials and minima of the (R–E) curve in Fig. 6. The corresponding non-monotonous behavior of the lithium ion diffusional characteristic and charge-transfer parameter can be ascribed to attractive interactions among the intercalated species in the cathode host material and phase transitions during Li-ion intercalation/deintercalation.

4. Conclusions

Electrochemical method of synthesis of vanadium oxides from aqueous vanadyl sulfate solution providing both its stable characteristics and predetermined properties of oxides has been developed.

On the basis of a complex investigation using physical and electrochemical methods, we have established and discussed the correlation between structural characteristics of the ESVO electrode, their electrochemical responses in terms of cyclic voltammetry, impedance spectroscopy and chronopotentiometry, and the dependence of the chemical diffusion coefficient of Li-ions on the state-of-discharge.

Acknowledgements

This work was supported by the Ministries of Science of Ukraine and of the State of Israel in the framework of the joint Ukrainian-Israeli R&D project 2M/1420-97. The authors would like to thank Prof. M. Valakh in assistance for Auger-electron spectroscopy measurements.

References

[1] N. Kumagai, K. Tanno, Denki Kagaku 48 (1980) 432.
[2] N. Kumagai, K. Tanno, T. Nakajima, N. Watanabe, Electrochim. Acta 28 (1983) 17.
[3] D.W. Murphy, P.A. Cristian, F.J. DiSalvo, J.N. Caride, J. Electrochem. Soc. 126 (1970) 497.
[4] K.M. Abraham, J.L. Goldman, M.D. Dempsey, J. Electrochem. Soc. 128 (1981) 2493.
[5] D.B. Le, S. Passerini, J. Guo, J. Ressler, B.B. Owens, W.H. Smyrl, J. Electrochem. Soc. 143 (1996) 2099.
[6] S.-I. Ryun, J.-S. Bae, J. Power Sources 68 (1997) 669.
[7] X. Zhang, R. Frech, Electrochim. Acta 42 (1997) 475.
[8] N. Kumagai, H. Kitamoto, M. Baba, S. Durand-Vidal, D. Devilliers, H. Groult, J. Appl. Electrochem. 28 (1998) 41.
[9] J.P. Pereira-Ramos, R. Messina, C. Piolet, J. Devynck, Electrochim. Acta 33 (1988) 1003.
[10] Y. Sato, T. Asada, H. Tokugawa, K. Kobayakawa, J. Power Sources 68 (1997) 674.
[11] J.P. Pereira-Ramos, R. Messina, C. Piolet, J. Devynck, J. Power Sources 20 (1987) 221.
[12] E. Andrukaitis, E.A. Bishenden, P.W.M. Jacobs, J.W. Lorimer, J. Power Sources 26 (1989) 475.
[13] K. West, B. Zachau-Christiansen, T. Jacobsen, Electrochim. Acta 28 (1983) 1829.
[14] K. West, B. Zachau-Christiansen, T. Jacobsen, J. Power Sources 43–44 (1993) 127.
[15] J.-I. Yamaki, S.-I. Tobishima, Y. Sakurai, K.-I. Saito, K. Hayashi, J. Appl. Electrochem. 28 (1998) 135.
[16] S.-I. Tobishima, K. Hayashi, K. Saito, T. Shodai, J.-I. Yamaki, Electrochim. Acta 42 (1997) 119.
[17] K. West, B. Zachau-Christiansen, S. Skaarup, Y. Saidi, J. Barker, I.I. Olsen, R. Pynenburg, R. Koksbang, J. Electrochem. Soc. 143 (1996) 820.
[18] M.G. Minett, J.R. Owen, J. Power Sources 32 (1990) 81.
[19] K. West, B. Zachau-Christiansen, M.J.L. Ostergard, T. Jacobsen, J. Power Sources 20 (1987) 165.
[20] H.-K. Park, W.H. Smyrl, M.D. Ward, J. Electrochem. Soc. 142 (1995) 1068.
[21] U. Von Sacken, J.R. Dahn, J. Power Sources 26 (1989) 461.
[22] N. Machida, R. Fuchida, T. Minami, J. Electrochem. Soc. 136 (1989) 2133.
[23] R.D. Apostolova, V.M. Nagirny, E.M. Shembel, Proc. 190th Electrochem. Soc. Meeting, San Antonio, Oct., 6–11, 1996, Abstr. No. 131, 178.
[24] V.M. Nagirny, N.I. Globa, N.D. Zadereiy, B.I. Melnikov, E.M. Shembel, Proc. Joint Int. Electrochem. Soc. Meeting, Paris, Aug. 31–Sept. 5, 1997, Abstr. 911, 1096.
[25] Y. Sakurai, S. Okada, J. Yamaki, T. Okada, J. Power Sources 20 (1987) 173.
[26] Y. Sato, T. Nomura, H. Tanaka, K. Kobaykawa, Electrochem. Soc. Lett. 138 (1991) L37.
[27] K. Wiesener, W. Schneider, D. Ilic, E. Steger, K.H. Hallmeier, E. Brackman, J. Power Sources 20 (1987) 157.

[28] S. Hub, A. Tranchant, R. Messina, J. Electrochim. Acta 33 (1988) 997.
[29] X. Zhang, R. Frech, J. Electrochem. Soc. 145 (1998) 847.
[30] J.M. Cocciantelli, J.P. Doumerc, M. Pouchard, M. Broussely, J. Labat, J. Power Sources 34 (1991) 103.
[31] W. Weppner, R.A. Huggins, Ann. Rev. Mater. Sci. 8 (1978) 269.
[32] C. Ho, I.D. Raistrick, R.A. Huggins, J. Electrochem. Soc. 127 (1980) 343.
[33] D. Aurbach, M.D. Levi, J. Phys. Chem. B 101 (1997) 4641.
[34] D. Aurbach, M.D. Levi, E. Levi, B. Markovsky, G. Salitra, H. Teller, U. Heider, V. Hilarius, Proc. Electrochem. Soc. 97 18 (1997) 941.
[35] D. Aurbach, M.D. Levi, B. Markovsky, H. Teller, G. Salitra, J. Electrochem. Soc. 145 (1998) 3024.
[36] S. Yamada, M. Fujiwara, M. Kanda, J. Power Sources 54 (1995) 209.